Electronic Structure of Transition-Metal Nitrosyls. Xα–SW and Configuration Interaction Calculations of the Valence Ionization Potentials of $Co(CO)_3NO$ and $Mn(CO)_4NO$

Bruce E. Bursten, J. Robert Jensen, Douglas J. Gordon, Paul M. Treichel, and Richard F. Fenske*

Contribution from the Department of Chemistry, University of Wisconsin, Madison, Wisconsin 53706. *Received January 12, 1981*

Abstract: Projected Xα–SW and configuration interaction calculations are used to discuss the bonding and photoelectron spectra of $Co(CO)_3NO$ and $Mn(CO)_4NO$, the latter spectrum being reported for the first time. Ionization potentials are obtained from the correlated wave function by using the extended Koopmans' theorem method of Smith and Day, the first application of this formalism or the equivalent one of Morrel, Parr, and Levy to transition-metal systems. Both the Xα–SW and CI predicted ionization potentials are far more reasonable than those of Hartree–Fock as predicted by Koopmans' theorem, and the calculations generally support the notion that the electronic structure of the nitrosyl complexes may be derived as a symmetry lowering of $Ni(CO)_4$ or $Fe(CO)_5$. A conjecture is offered as to the reason for the apparent success of approximate MO methods over that of ab initio Hartree–Fock calculations on transition-metal systems.

The growth of photoelectron spectroscopy (PES) as a probe of the electronic structure of molecules has provided a stringent test of electronic structure calculational theories. The early success of single configuration Hartree–Fock calculations and Koopmans' theorem[1] when applied to first-row diatomic molecules and organic systems was quite promising and spurred more ambitious investigations on larger systems, in particular those containing transition-metal atoms. It has been found, however, that there are often gross differences between the observed ionization energies and those predicted by Koopmans' theorem.[2]

In recent years, the sources of the apparent failure of Koopmans' theorem for transition-metal systems have come under closer scrutiny. Veillard and Benard at Strasbourg have noted that the inclusion of limited configuration interaction (CI) to Hartree–Fock calculations on quadruply bonded metal–metal systems produces large changes in the predicted ground-state electronic structure.[3,4] For example, while the Hartree–Fock calculation on $Cr_2(O_2CH)_4$ yields a configuration corresponding to no net metal–metal bond,[5] it is found that the correlated wave function corresponds more closely to strong metal–metal bonding between the Cr atoms, a result that had been predicted by both a qualitative overlap model[6] and by more quantitative Xα–SW calculations.[7] The latter results may be further refined by the inclusion of valence bond concepts to improve the energetics without drastically changing the bonding picture.[8]

Interest in our laboratories has focused on the comparison of the carbonyl and nitrosyl moieties as terminal ligands for transition metals.[2,9,10] These studies have increased importance in view of the recent growth in the photochemistry of $Co(CO)_3NO$[11] and $Mn(CO)_4NO$[12] and in the chemistry of organometallic nitrosyl complexes.[13] It had been predicted via nonempirical MO calculations that the isoelectronic CO and NO^+ groups are qualitatively similar in their bonding to metals.[2] Seemingly in support of this, the PE spectra of $Ni(CO)_4$ and $Co(CO)_3NO$ are nearly indistinguishable.[14] However the Hartree–Fock calculations on these two systems yield entirely different results.[14] Analogous differences are apparent in the isoelectronic molecules $Fe(CO)_5$ and $Mn(CO)_4NO$; i.e., according to a Hartree–Fock calculation the orbital structure of the latter cannot be treated as a simple perturbation of the former.[15] In an effort to ascertain whether or not these large differences are real, it is necessary to go beyond a single configuration wave function for these systems. In an earlier paper from this laboratory, Fenske and Jensen have reported CI calculations on $Co(CO)_3NO$ and $Mn(CO)_4NO$.[10] The results were quite striking; in both cases, the inclusion of correlation greatly changed the charge density about the metal atom, yielding a more spherical distribution than that obtained at the single configuration level. It would appear, therefore, that, as in the case of $Cr_2(O_2CH)_4$, a multiconfiguration wave function is necessary to adequately describe the electronic structure of these transition-metal–nitrosyl complexes.

In this paper, we will report our continued studies of the electronic structure of metal–nitrosyl complexes. The Fenske–Jensen[10] correlated wave functions for $Co(CO)_3NO$ and $Mn(CO)_4NO$ are used in conjunction with the extended Koopmans' theorem formalism developed by Smith and Day[16–19] to obtain theoretical ionization energies from the general ground-state CI calculations. This is, to our knowledge, the first application of such a formalism to transition-metal systems. These energies are compared to those obtained from Xα–SW calculations on the two molecules. Analysis of the Xα–SW molecular orbitals has been achieved by using our projected Xα (PXα) method[20] in order to

---

(1) Koopmans, T. *Physica*, **1934**, *1*, 104–113.
(2) Fenske, R. F. *Prog. Inorg. Chem.* **1976**, *21*, 179–208.
(3) Bênard, M.; Veillard, A. *Nouv. J. Chim.* **1977**, *1*, 97–99.
(4) Bênard, M. *J. Chem. Phys.* **1979**, *71*, 2546–2556.
(5) Garner, C. D.; Hillier, I. H.; Guest, M. F.; Green, J. C.; Coleman, A. W. *Chem. Phys. Lett.* **1976**, *41*, 91–94.
(6) Cotton, F. A. *Inorg. Chem.* **1965**, *4*, 334–336.
(7) Cotton, F. A.; Stanley, G. G. *Inorg. Chem.* **1977**, *16*, 2668–2671.
(8) Noodleman, L.; Norman, J. G., Jr. *J. Chem. Phys.* **1979**, *70*, 4903–4906.
(9) Jensen, J. R.; Fenske, R. F. *Theor. Chim. Acta*, **1978**, *48*, 241–249.
(10) Fenske, R. F.; Jensen, J. R. *J. Chem. Phys.* **1979**, *71*, 3374–3382.
(11) Evans, W. E. Ph.D. Thesis, University of California, Los Angeles, 1979.
(12) Keeton, D. P.; Basolo, F. *Inorg. Chim. Acta* **1972**, *6*, 33–38.
(13) See, for example, the series by Legzdins and co-workers, the most recent of which is: Hames, B. W.; Kolthammer, B. W. S.; Legzdins, P. *Inorg. Chem.* **1981**, *20*, 650–656.
(14) Hillier, I. H.; Guest, M. F.; Higginson, B. R.; Lloyd, D. R. *Mol. Phys.* **1974**, *27*, 215–223.
(15) Jensen, J. R. Ph.D. Thesis, University of Wisconsin, Madison, 1978.
(16) Day, O. W.; Smith, D. W.; Garrod, C. *Int. J. Quantum Chem. Symp.* **1974**, *8*, 501–509.
(17) Smith, D. W.; Day, O. W. *J. Chem. Phys.* **1975**, *62*, 113–114.
(18) Day, O. W.; Smith, D. W.; Morrison, R. C. *J. Chem. Phys.* **1975**, *62*, 115–119.
(19) Morrison, R. C.; Day, O. W.; Smith, D. W. *Int. J. Quantum Chem. Symp.* **1975**, *9*, 229–235.
(20) Bursten, B. E.; Fenske, R. F. *J. Chem. Phys.* **1977**, *67*, 3138–3145.

0002-7863/81/1503-5226$01.25/0

avoid the ambiguities of contour maps or atomic sphere population analysis.[21] These results will be compared to the PE spectra of $Co(CO)_3NO$ and $Mn(CO)_4NO$, the latter being reported for the first time.

Experimental and Calculational Details

Photoelectron Spectrum of $Mn(CO)_4NO$. $Mn(CO)_4NO$ was prepared by the method of Treichel et al.[22] The compound was characterized by its deep red color and by its infrared spectrum, which indicated no traces of $Mn(CO)_5H$ in the sample. The photoelectron spectrum was obtained by using a Varian IEE-15 spectrometer in the UV configuration. Argon was used as a single internal standard. The sample was introduced through the variable-temperature inlet system, and the spectrum was taken at ambient temperature. Multiple scans were used to improve the signal-to-noise ratio and to monitor sample decomposition. The reported spectrum is the sum of 25 individual time averaged sweeps of 100-s duration across a 10-eV region. Sample decomposition was noted, as several very sharp peaks started to grow in after ~10 scans.

CI Calculations. The atomic basis sets used for the cobalt and manganese atoms are contractions of the Gaussian atomic orbitals of Roos et al.[23] The carbon, nitrogen, and oxygen bases are Pople's 3G-STO constrained atomic functions.[24] The geometries of $Co(CO)_3NO$ and $Mn(CO)_4NO$ were taken from the diffraction studies of Brockway et al.[25] and Frenz et al.,[26] respectively, and were idealized to C_{3v} and C_{2v} point symmetries.

The energy-based-integral-retention (EBIR) method[27] was used to reduce the number of integrals while guaranteeing accurate Hartree–Fock and CI results. A value of 1×10^{-3} au was used as a threshold for integral evaluation for both molecules and in each case this results in a reduction of the number of integrals by approximately a factor of 3. For each molecule a two-pass, iterative natural orbital CI calculation was performed, as previously described.[10]

Ionization energies were obtained from the correlated wave functions through application of the extended Koopmans' theorem formalism, which is discussed in the Appendix.

Xα–SW Calculations. The scattered-wave Xα molecular orbital method developed by Slater and Johnson[28] was also used to calculate the electronic structure of $Co(CO)_3NO$ and $Mn(CO)_4NO$. The same idealized coordinate systems used for the CI calculations were used for the Xα–SW calculations. The starting potential was derived from a superposition of neutral, Herman–Skillman[29] atomic charge densities. The α_{HF} values from the compilation of Schwarz[30] were used for both the atomic and molecular calculations.

Sphere radii for the atoms were taken to be 87% of the atomic charge radius from the atomic density superposition. The sphere radii for $Co(CO)_3NO$ (in atomic units) were as follows: outer sphere, 7.182, Co, 2.142; N, 1.571; O_N, 1.600; C, 1.611; O_C, 1.627. Those for $Mn(CO)_4NO$ were as follows: outer sphere, 7.339; Mn, 2.183; N, 1.573; O_N, 1.591; C_{eq}, 1.620; O_{eq}, 1.630; C_{ax}, 1.620; O_{ax}, 1.620. These values are found to satisfactorily conform with Norman's nonempirical criterion for sphere radius choice.[31]

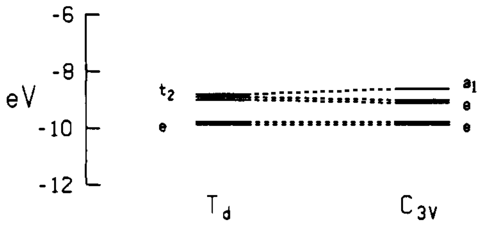

Figure 1. Splitting of the valence levels on reduction from T_d to C_{3v} symmetry.

Table I. PXα Orbital Energies, Transition-State Ionization Potentials, and Mulliken Percent Characters of the 11e, 12e, and 17a Molecular Orbitals of $Co(CO)_3NO$

		predicted	Co[a]			NO[a]		CO	
orbital	ϵ, eV	IP, eV	3d	4s	4p	5σ	2π	5σ	2π
$17a_1$[b]	−4.60	7.16	64	0	15	5	-	2	12
12e	−4.94	7.39	48	-	19	-	18	6	7
11e	−6.20	8.91	76	-	0	-	14	0	2

[a] Percent character contributions indicated by a dash are zero by symmetry. [b] Highest occupied orbital of the complex.

The Slater orbital basis used in the PXα calculations was chosen for maximum overlap with the Herman–Skillman atomic radial functions.[32] Double-ζ metal 3d and ligand 2p STO's were used; all other basis orbitals were single ζ. The quadrature used for both molecules consisted of 25 radial points, nine θ points, and 18 ϕ points. The results were transformed into the PXα MO's for CO and NO^+; for both of these, the 6σ orbital was determined by Schmidt orthogonalization to the 3σ, 4σ, and 5σ orbitals.

Results and Discussion

$Co(CO)_3NO$. Although $Co(CO)_3NO$ is the simplest mononitrosyl complex, its electronic structure has been the subject of much debate. The molecule is often considered as a perturbation of isoelectronic $Ni(CO)_4$, wherein the perturbation is the transfer of a nuclear charge from the nickel to the carbon. If this perturbation is regarded as having a small effect on the valence levels, a qualitative description of the electronic structure of $Co(CO)_3NO$ can be attained by breaking the symmetry of the $Ni(CO)_4$ orbitals. Upon reduction from T_d to C_{3v} point symmetry, the primarily metal t_2 orbitals will split as $a_1 + e$, while the metal e orbitals remain degenerate (see Figure 1). In order to distinguish the two sets of e orbitals, we will label them e_t or e_e depending on their origin from T_d symmetry. If the change in symmetry is a small perturbation, it is expected that the a_1 and e_t orbitals would be nearly degenerate. Indeed, there is a great similarity in the valence photoelectron spectra of $Ni(CO)_4$ and $Co(CO)_3NO$.[14] The 8–11-eV ionization region for both molecules shows two bands of approximate relative intensity 3:2, the higher intensity band having a lower ionization potential. No splitting of the first ionization band of $Co(CO)_3NO$ is apparent. Thus, on the basis of the PE spectra, it would seem that there is a good transferability of the $Ni(CO)_4$ orbitals to $Co(CO)_3NO$. The Hartree–Fock calculations on the two molecules yield entirely different results, however.[14] From Koopmans' theorem, the first ionization is from an e orbital at 8.7 eV followed by a_1 and e ionizations at 12.9 and 14.1 eV, respectively. Furthermore, the spatial characters of the two sets of e orbital do not correspond to the e_t and e_e sets derived from T_d symmetry; rather the e sets correspond closely to the primarily metal π and δ sets of orbitals of the $C_{\infty v}$ fragment CoNO, with the π set, quite surprisingly, corresponding to the first ionization. This implies that the replacement of a carbonyl by a nitrosyl is quite a drastic change and would seem to preclude the use of simple perturbation arguments (i.e., chemical intuition) in cor-

---

(21) Bursten, B. E.; Freier, D. G.; Fenske, R. F. *Inorg. Chem.* **1980**, *19*, 1810–1811.

(22) Treichel, P. M.; Pitcher, E.; King, R. B.; Stone, F. G. A. *J. Am. Chem. Soc.* **1961**, *83*, 2593–2594.

(23) Roos, B.; Veillard, A.; Vinot, G. *Theor. Chim. Acta* **1971**, *20*, 1–11.

(24) Ditchfield, R.; Hehre, W. J.; Pople, J. A. *J. Chem. Phys.* **1970**, *52*, 5001–5007.

(25) Brockway, L. O.; Anderson, J. S. *Trans. Faraday Soc.* **1937**, *33*, 1233–1239.

(26) Frenz, B. A.; Enemark, J. H.; Ibers, J. A. *Inorg. Chem.* **1969**, *8*, 1288–1293.

(27) Jensen, J. R.; Fenske, R. F. *J. Chem. Phys.* **1978**, *69*, 912–917.

(28) Slater, J. C. "Quantum Theory for Molecules and Solids: The Self-Consistent Field for Molecules and Solids"; McGraw-Hill: New York, 1974; Vol. 4.

(29) Herman, F.; Skillman, S. "Atomic Structure Calculations"; Prentice-Hall: Englewood Cliffs, N.J., 1963.

(30) Schwarz, K. *Phys. Rev. B* **1972**, *5*, 2466–2468.

(31) Norman, J. G., Jr. *Mol. Phys.* **1976**, *31*, 1191–1198.

(32) Bursten, B. E.; Jensen, J. R.; Fenske, R. F. *J. Chem. Phys.* **1978**, *68*, 3320–3321.

(33) Mulliken, R. S. *J. Chem. Phys.* **1955**, *23*, 1833–1840.

relating the spectra of different but related compounds. It is also apparent that Koopmans' theorem predicts a much larger spread (~5.4 eV) in the metal-based ionizations than that found experimentally (~0.9 eV). Thus there are three dissatisfying features in the Hartree–Fock calculation on $Co(CO)_3NO$: (1) the greater transferability of the $C_{\infty v}$ orbitals of CoNO than the T_d orbitals of $Ni(CO)_4$, (2) the nonintuitive ordering of the three metal-based ionizations, and (3) the very large spread in the ionizations. These three points will be the focus of our discussion of the PXα and CI calculations on the molecule.

The PXα orbital energies, transition-state ionization potentials and Mulliken percent characters[33] of the 11e, 12e, and 17a$_1$ levels of $Co(CO)_3NO$ are given in Table I. These three molecular orbitals are the highest occupied MO's in the complex and are the only filled orbitals with appreciable metal character. Several features are notable. With the assumption that the first three ionization cross sections of $Co(CO)_3NO$ are about equal and that the 12e and 17a$_1$ ionizations could not be resolved, the PE spectrum would be expected to have two bands in approximately a 3:2 intensity ratio. This is in accord with the observed spectrum. The predicted ionization potentials are uniformly too low, but the gap between the predicted IP's (~1.6 eV) is far closer to the experimental one of 0.9 eV than is that predicted by Koopmans' theorem (~5 eV). It is significant to note that there is substantial mixing between the e($d_{x^2-y^2}$,d_{xy}) and e(d_{xz},d_{yz}) sets of metal orbitals. This indicates that $Co(CO)_3NO$ is not well represented by quantization about the threefold axis, as might be expected if the Co–NO interaction dominated the bonding picture. Rather, the metal levels behave as if they were quantized according to T_d symmetry. With use of Ballhausen's convention,[34] the transformation from the axially quantized d orbitals to the tetrahedrally quantized d orbitals is

$$a_1 = d_{z^2}$$

$$e_t^+ = \sqrt{2/3}d_{x^2-y^2} - \sqrt{1/3}d_{xz}$$

$$e_t^- = \sqrt{2/3}d_{xy} + \sqrt{1/3}d_{yz}$$

$$e_e^+ = \sqrt{1/3}d_{x^2-y^2} + \sqrt{2/3}d_{xz}$$

$$e_e^- = \sqrt{1/3}d_{xy} - \sqrt{2/3}d_{yz}$$

where e$_t$ is the e set obtained from the T_d t$_2$ metal orbitals upon reduction of symmetry and e$_e$ is identical with the e set of T_d symmetry. When the PXα results are transformed into the tetrahedrally quantized orbitals, it is found that the 11e MO is 76% e$_e$ and <1% e$_t$ while the 12e MO is 41% e$_t$ and 7% e$_e$. This is quite a satisfying result since it implies a transferability of orbital character from $Ni(CO)_4$ to $Co(CO)_3NO$; i.e., the influence of the nitrosyl is not so great as to force a rehybridization of the metal orbitals. As in $Ni(CO)_4$ there are significant ligand π contributions to all of the primarily metal orbitals, although the nitrosyl is clearly a better π acceptor than are the carbonyls. This point is underscored by the total orbital Mulliken populations for $Ni(CO)_4$ and $Co(CO)_3NO$, reported in Table II.

The greater π-accepting ability of nitrosyls relative to carbonyls is indirectly responsible for the intuitively displeasing Hartree–Fock picture of $Co(CO)_3NO$, for it results in a large one-center splitting of the Co 3d orbitals (cf. Figure 5 of ref 10). The source of this splitting has been attributed to the distribution of electron density on the metal atom rather than the electrostatic ligand field.[9] Our earlier work[10] has demonstrated that the inclusion of CI greatly reduces the charge asymmetry about the Co atom and that, furthermore, the quantization of the Co AO's is better described as tetrahedral rather than axial. It is desirable, therefore, to obtain ionization potentials from the correlated wave function in order to assess whether the energetics also change upon the inclusion of correlation and for comparison to the Xα results. IP's have been obtained in two fashions. First, the extended Koopmans' theorem (EKT) formalism has been used to obtain IP's directly from the neutral molecule ground-state CI wave functions. Second, a CI calculation on the ground state of $[Co(CO)_3NO]^+$ allows evaluation of the first IP by total energy difference (the ΔCI method).

Table II. PXα Mulliken Populations for $Ni(CO)_4$, $Co(CO)_3NO$, and $Mn(CO)_4NO$[a]

				$Ni(CO)_4$					
Ni:	e	t$_2$	4s	4p	CO:	5σ	2π		
	3.71	5.18	0.45	0.84		1.68	0.27		
				$Co(CO)_3NO$					
Co:	e$_e$	e$_t$	a$_1$	4s	4p	NO:	5σ	2π	
	3.48	2.77	1.64	0.35	1.20		1.78	1.31	
CO:	5σ	2π							
	1.56	0.28							
				$Mn(CO)_4NO$[b]					
Mn:	z^2	x^2-y^2					NO:	5σ	2π
	1.25	0.88	1.66	1.44	1.14	0.53		1.83	1.31
CO$_{eq}$:	5σ	2π		CO$_{ax}$:	5σ	2π			
	1.63	0.48			1.65	0.25			

[a] Ligand populations are for a single ligand. [b] No 4p AO's were included on the Mn in $Mn(CO)_4NO$.

Table III. Calculated and Observed Ionization Potentials for $Co(CO)_3NO$ (in eV)[a]

Hartree–Fock[b]	Xα	CI(EKT)	CI(ΔCI)	exptl[c]
6.4 (^{2}E)	7.2 (^{2}A$_1$)	8.4 (^{2}E)	8.0 (^{2}E)	8.9
11.4 (^{2}A$_1$)	7.4 (^{2}E)	8.6 (^{2}A$_1$)		9.8
12.4 (^{2}E)	8.9 (^{2}E)	10.2 (^{2}E)		

[a] Final states of the ionized molecule given in parentheses.
[b] Koopmans' theorem IP from the leading configuration of ref 10.
[c] Reference 14.

The EKT formalism,[16-19] described in the Appendix, allows the calculation of a spectrum of first-order ionization potentials for arbitrary wave functions. The EKT IP's calculated for the two pass CI wave function of $Co(CO)_3NO$ are compared to Koopmans' theorem, the Xα transition state, and experimental IP's in Table III. It is seen that the EKT results are in excellent accord with experiment as it is predicted that the fist ionization band should be comprised of an a$_1$ and an e ionization with a second e ionization ~1.7 eV greater in energy. Although this separation is somewhat greater than that observed experimentally (~0.9 eV), it is clear that the most dissatisfying aspects of the Koopmans' theorem predictions, namely, the 5–6-eV gap between the first two ionization bands and the inconsistent intensity distribution, disappear upon inclusion of CI.

To provide a check on the EKT results, a CI calculation on the ground ^{2}E state of $[Co(CO)_3NO]^+$ has been performed. For the sake of comparison to the neutral molecule, the natural orbitals used to construct configurations for the cation were those used for the two pass CI wave function of our previous study.[10] The resulting CI wave function for $[Co(CO)_3NO]^+$ has an energy of −1842.404 au, 0.294 au above the ground state of the neutral molecule. Thus, the first IP is predicted to be 8.00 eV, about 0.9 eV lower than observed but substantially better than the 6.7 eV ΔSCP IP predicted at the single configuration level.[14] It is apparent that both methods detailed here for obtaining IP's from the CI wave functions yield results superior to those at the SCF level and far more physically pleasing.

A point yet to be considered is the character of the first ionization of $Co(CO)_3NO$ at the CI level. We recall that the Xα–SW method predicts the first e ionization corresponds to the removal of primarily e$_t$ metal electrons in analogy with the first ionization of $Ni(CO)_4$. The nonempirical Fenske–Hall method has arrived at a similar conclusion.[2] The nature of the first IP at the CI level has been determined by comparing the Mulliken populations of

---

(34) Ballhausen, C. J. "Introduction to Ligand Field Theory"; McGraw-Hill: New York, 1962.

Table IV. Mulliken Populations of the Pertinent Co and NO Orbitals from the CI Calculations on $Co(CO)_3NO$ and $[Co(CO)_3NO]^+$

orbital	$Co(CO)_3$-NO	$[Co(CO)_3$-$NO]^+$	Δ
Co e_t	1.55	1.55	0.00
Co e_e	0.96	0.75	0.21
NO 2π	0.82	0.24	0.58

pertinent orbitals for the neutral molecule and the cation (Table IV). It is seen that in the course of ionization to $[Co(CO)_3NO]^+$, the most density is lost from the nitrosyl 2π orbitals and that the Co density comes from e_e rather than from e_t orbitals. Thus the picture of the ionization given by the CI calculation more closely compares to that of the Hartree–Fock method than to the Xα–SW calculation. It would therefore seem that the PE spectrum of $Co(CO)_3NO$ is not a simple product of symmetry lowering of the spectrum of $Ni(CO)_4$, although it must be remembered that the ΔCI method yields a "totally relaxed" ionization and that the two e levels may mixt upon relaxation. We shall see that this problem is circumvented in the study of $Mn(CO)_4NO$.

$Mn(CO)_4NO$. $Mn(CO)_4NO$ can also be considered as a perturbation of an isoelectronic metal carbonyl, in this case $Fe(CO)_5$. The two highest occupied orbitals in $Fe(CO)_5$ are the primarily metal 10e′ and 3e″. Upon a reduction from D_{3h} to C_{2v} symmetry, the e′ orbital will split as $a_1 + b_2$ while the e″ will split as $a_2 + b_1$. Thus if the highest occupied orbitals of $Mn(CO)_4NO$ can be described as a perturbation of those of $Fe(CO)_5$, one would expect two groups of two orbitals, the a_1 and b_2 pair higher in energy than the a_2 and b_1 pair.

As was the case for $Co(CO)_3NO$, the PE spectrum of $Mn(CO)_4NO$ seems supportive of these arguments. The PE spectrum of $Fe(CO)_5$ shows two peaks of virtually the same intensity in the metal ionization region.[35] The first vertical IP, at 8.60 eV, has been assigned to ionization from the 10e′ MO while the second vertical IP, at 9.86 eV, is assigned to the 3e″ MO. The equal intensity of these two bands is supportive of the assumption of nearly equal ionization cross sections for the metal electrons in these systems. The He I photoelectron spectrum of $Mn(CO)_4NO$, shown in Figure 2, shows three bands in the 8–10-eV ionization region, corresponding to vertical IP's of 8.4 (E_1), 9.1 (E_2), and 9.6 (E_3) eV, respectively. The onset of ligand ionizations at ~13 eV is typical of this type of compound.[14]

The intensity ratio E_1:E_2:E_3 is roughly 1:3:2, but the overlap of E_2 and E_3 makes an absolute intensity determination difficult to obtain. The spike on E_3, the structure in the 11.8–12.8-eV region, and the spikes at 13.5 and 14.8 eV were only evident after ~10 scans and are undoubtedly attributable to photodecomposition of $Mn(CO)_4NO$, which is known to be light sensitive.[22] Similar ionizations due to decomposition were observed in the PE spectrum of $Ni(CO)_4$.[14] Bands E_1, E_2, and E_3 were evident in the first scan with the observed intensity distribution, and we are therefore confident that they may be assigned to $Mn(CO)_4NO$.

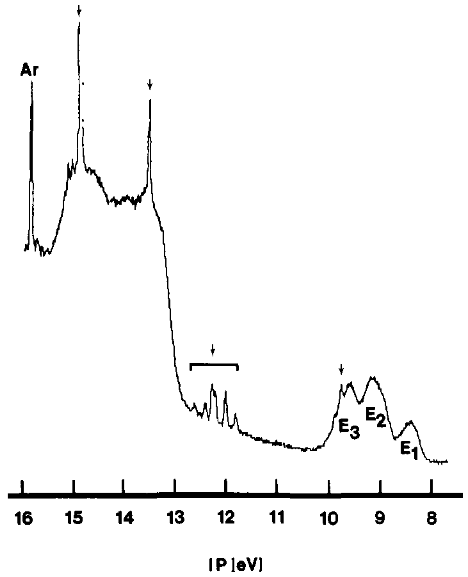

Figure 2. The He I photoelectron spectrum of gaseous $Mn(CO)_4NO$. The spectrum is the result of 25 individual scans of 100 s each. The peaks marked with arrows started growing in after ~10 scans and are due to photodecomposition of $Mn(CO)_4NO$.

Table V. PXα Orbital Energies, Transition-State Ionization Potentials, and Mulliken Percent Characters of the $11b_1$, $3a_2$, $11b_2$, and $23a_1$ Molecular Orbitals of $Mn(CO)_4NO$

		pre-dicted		NO^a		$CO_{eq}{}^a$		$CO_{ax}{}^a$	
orbital	ε, eV	IP, eV	Mn	5σ	2π	5σ	2π	5σ	2π
$23a_1{}^b$	−4.62	6.94	59^c	4	-	4	27	0	5
$11b_2$	−5.03	7.39	35	-	44	9	5	-	4
$3a_2$	−5.43	7.91	79	-	-	-	8	-	7
$11b_1$	−5.64	8.11	68	-	17	-	3	0	6

[a] Percent character contributions indicated by a dash are zero by symmetry. [b] Highest occupied orbital of the complex. [c] Mn 4s contribution to the $23a_1$ MO is negligible.

The PXα results for the four highest occupied orbitals of $Mn(CO)_4NO$ are summarized in Table V. It is seen that the ordering of levels agrees with the qualitative ordering derived above. The $23a_1$ HOMO is essentially a Mn $3d_{z^2-y^2}$ orbital stabilized by interaction with the equatorial carbonyl 2π orbitals. The $z^2 - y^2$ orbital in the coordinate system used for $Mn(CO)_4NO$ (z = Mn–N; $x = C_{ax}$–Mn) corresponds to the $x^2 - y^2$ orbital under D_{3h} symmetry, there is, as for $Co(CO)_3NO$, a transferability of those orbitals in the higher symmetry parent carbonyl. The $11b_2$ orbital represents a strong covalent interaction between the Mn $3d_{yz}$ AO (which corresponds to the $3d_{xy}$ orbital in $Fe(CO)_5$) and the nitrosyl 2π orbital in the equatorial plane. From a comparison of the characters of the $23a_1$ and $11b_2$ orbitals, it is apparent that the nitrosyl interacts with the metal more strongly than do the equatorial carbonyls. The $3a_2$ and $11b_1$ orbitals are fairly similar in character, consisting of the $3d_{xy}$ and $3d_{xz}$ AO's respectively interacting with both the axial and equatorial CO 2π orbitals. The $3d_{xz}$ AO also interacts strongly with the NO 2π orbital perpendicular to the equitorial plane, resulting in a stabilization of the $11b_1$ orbital relative to the $3a_2$. Total Mulliken populations of the pertinent orbitals are presented in Table II.

The agreement between the transition-state IP's and the experimental ones is quite good. Analogous to the earlier results for $Co(CO)_3NO$, the calculated IP's for $Mn(CO)_4NO$ are uniformly too low in value; the spacings between the ionizations are in excellent accord, however. E_1 is assigned to ionization from the $23a_1$ MO, E_2 is assigned to the $11b_2$ orbital, and E_3 is assigned to both the $3a_2$ and $11b_1$ MO's; i.e. the splitting of the 3e″ orbital of $Fe(CO)_5$ is not great enough to be observed. The predicted differences between E_1 and E_2 (0.46 eV) and between E_2 and E_3 (0.62 eV) compare most favorably with the experimental differences of 0.66 and 0.54 eV, respectively. The only disturbing aspect of this assignment is that the intensity of E_3 would presumably be expected to be greater than that of E_2 since the former is composed of two ionizations.

Before discussing the EKT results for $Mn(CO)_4NO$, it is instructive to reiterate the differences between the SCF and CI wave functions as reported in our previous work.[10] The Hartree–Fock calculation on $Mn(CO)_4NO$ yielded a tremendous charge asymmetry about the Mn–NO bond. The nitrosyl is predicted to interact only in the equatorial plane as the NO $2\pi_y$ orbital is split ~11 eV lower than the $2\pi_x$ orbital. In fact, the $2\pi_y$ is ~8 eV *lower* than the Mn $3d_{yz}$ AO and the orbital which results from this interaction, the $11b_2$ MO, is predominantly NO 2π in

---

(35) Lloyd, D. R.; Schlag, E. W. *Inorg. Chem.* **1969**, *8*, 2544–2555.

Table VI. Calculated and Observed Ionization Potentials for $Mn(CO)_4NO$ (in eV)[a]

Hartree–Fock[b]	Xα	CI(EKT)	exptl
7.5 ($^2B_2$)	6.9 ($^2A_1$)	8.2 ($^2A_1$)	8.4
9.8 ($^2A_1$)	7.4 ($^2B_2$)	8.9 ($^2B_2$)	9.1
11.2 ($^2A_2$)	7.9 ($^2A_2$)	9.0 ($^2A_2$)	
11.5 ($^2B_1$)	8.1 ($^2B_1$)	10.1 ($^2B_1$)	9.6

[a] Final states of the ionized molecule given in parentheses.
[b] Koopmans' theorem IP from the leading configuration of ref 10.

character, a description more appropriate for a bent NO (often represented as NO^-) than for a linear NO. The total Mulliken populations of the Mn $3d_{xz}$ (1.74 e) and the Mn $3d_{yz}$ (0.29 e) reflect this asymmetry. The Koopmans' theorem IP's, given in Table VI, predict ~4 eV between the lowest and the highest metal-based ionizations, more than 3 times greater than observed.

Inclusion of CI greatly changes the picture. The orbitals of b_2 and b_1 symmetry are seen to correlate most strongly, and these are precisely the symmetries of the Mn–NO 2π interactions. The effect of this correlation is to greatly reduce the asymmetry about the Mn atom; after the second pass of CI, the Mulliken populations of the Mn $3d_{xz}$ and $3d_{yz}$ orbitals are 1.41 and 0.78 e, respectively. These compare well with the PXα Mulliken populations reported in Table II. The effect of CI upon the predicted IP's is quite dramatic as well. The EKT predicted IP's, presented in Table VI, are in excellent agreement with experiment. The ordering of the IP's is the same as that predicted by Xα although it is seen that the splitting pattern is somewhat different. E_1 is still assigned to a_1 symmetry, but E_2 is now assigned to ionization of both a_2 and b_2 symmetry while E_3 is assigned to a b_1 ionization. This assignment seems more consistent with the observed intensity distribution than does that predicted by Xα, although the difference between the two rests solely on the placement of the a_2 ionization. The present assignment also suggests that the asymmetry of E_2 may be due to a shoulder on the low-energy side. Attempts to resolve this shoulder were unsuccessful. It is interesting to note that the difficulties encountered for $Co(CO)_3NO$ by having two ionizations of e symmetry have been nicely circumvented in $Mn(CO)_4NO$, for the four ionizations of interest each correspond to different irreducible representations of C_{2v} symmetry. It is apparent that for $Mn(CO)_4NO$ that Xα and CI results are in essential agreement that the molecule may be considered as a symmetry lowering of $Fe(CO)_5$.

Conclusion

The studies presented in our earlier paper[10] and here provide a firm basis for the use of intuitive symmetry arguments in describing the bonding and energetics of the metal–nitrosyl interaction. As was the case for metal–metal quadruply bonded systems, it is clear that the single configuration wave function provides a woefully inadequate description of the bonding. The work presented here represents, to our knowledge, the first application of an extended Koopmans' theorem formalism to large transition-metal systems. It has been demonstrated not only that the inclusion of correlation leads to a more reasonable charge distribution for $Co(CO)_3NO$ and $Mn(CO)_4NO$ than does a single configuration wave function but also that remarkably accurate ionization potentials may be predicted as well. The EKT formalism should be generally applicable to any correlated wave function and, as the number of CI and MCSCF calculations on transition metal systems increases, it should prove most valuable in assigning PE spectra, especially for those systems in which there is disagreement between approximate and ab initio calculations.

The Xα studies presented here are yet another example of an approximate method providing a better description of the bonding and energetics of transition-metal systems than does Hartree–Fock theory. The charge densities and ionization potentials predicted by the Xα method compare very favorably with the much more expensive and computationally demanding CI calculations, although there is still a question concerning the assignment of the first ionization of $Co(CO)_3NO$. The consistency with which the Xα–SW, Fenske–Hall,[36] and extended Hückel[37] methods give results superior to those of Hartree–Fock on transition-metal systems is astounding, and we believe that these methods work *because of* the approximations made rather than *in spite of* them. On the basis of CI calculations, from this and other laboratories, we will conjecture as to the primary basis of the success of these approximate methods. In general it has been observed that Hartree–Fock calculations on low-symmetry transition-metal systems lead to a charge asymmetry about the metal atom. This effect is noted as well in high-symmetry species if the electron density is induced to be of lower symmetry than the nuclear framework,[4,10] i.e. the Hartree–Fock solutions are often unstable with respect to a lower symmetry solution. The inclusion of correlation generally restores much of the sphericity about the metal atom and, as has been demonstrated here, changes the energetics as well. Each of the three approximate methods mentioned above employs spherical averaging of the potential about the metal atom, and it is our belief that this averaging leads to charge distributions (and, by analogy, energetics) which more closely mimic those of a correlated wave function than of a Hartree–Fock single configuration wave function. Results from these laboratories[15] indicate that the spherical averaging restriction in the Fenske–Hall method may be lifted to yield solutions which are spatially and energetically very similar to those of Hartree–Fock. It is an interesting historical observation that for each of these approximate methods, the use of spherical averaging was for convenience rather than for rigor and that, in the case of Xα–SW, the spherical averaging has proven one of the most common sources of criticism with the method.

Acknowledgment. This research was supported by the National Science Foundation, Grant CHE75-17744, and by the Procter and Gamble Co. through a fellowship to B.E.B.

Appendix

Methods for obtaining ionization potentials from a general ground-state wave function were derived independently and concurrently by Smith and Day,[16,17] through the use of a second quantization formalism, and by Morrell, Parr and Levy (MPL),[38,39] through examination of the asymptotic behavior of the natural spin orbitals. The two formulations are entirely equivalent via transformation. The results presented in this paper have followed the extended Koopmans' theorem (EKT) approach of Smith and Day.

In the second quantization formalism we define creation and annihilation operators a_i^+ and a_i which create and annihilate, respectively, a particle in state ϕ_i. For fermions, these operators obey the anticommutation rules

$$\{a_i, a_j^+\} = \delta_{ij} \qquad \{a_i, a_j\} = \{a_i^+, a_j^+\} = 0$$

and their effect on a many electron wave function may be written as

$$a_i\psi^N(r_1, r_2, ..., r_N) = \int \mathrm{d}\tau_\mathrm{N}\phi_i(r_N)\psi^N(r_1, r_2, ..., r_N)$$

$$a_i^+\psi^N(r_1, r_2, ..., r_\mathrm{N}) = \mathcal{A}[\phi_i(r_{N+1})\psi^N(r_1, r_2, ..., r_N)]$$

where $\mathcal{A}$ is the antisymmetrizer.

Given a complete set of orbitals $\{\phi_i\}$, the $N - 1$ particle wave function in state s can be written as

$$\psi_\mathrm{s}^{N-1} = \sum_i C_{\mathrm{s}i}a_i\psi^N + \sum_{jkl} d_{\mathrm{s}jkl}a_\mathrm{j}a_k^+a_l\psi^N + ...$$

---

(36) Hall, M. B.; Fenske, R. F. *Inorg. Chem.* **1972**, *11*, 768–775.

(37) Hoffmann, R.; Lipscomb, W. N. *J. Chem. Phys.* **1962**, *36*, 2179–2189, 3489–3493.

(38) Morrell, M. M.; Parr, R. G.; Levy, M. *J. Chem. Phys.* **1975**, *62*, 549–554.

(39) Levy, M.; Parr, R. G. *J. Chem. Phys.* **1976**, *64*, 2707–2708.

In all that follows, it is assumed that only the first term need be kept, i.e., that "first order" ionizations will lead to wave functions

$$\psi_s^{N-1} = \sum_i C_{si} a_i \psi^N = A_s \psi^N \qquad A_s = \sum_i C_{is} a_i \tag{1}$$

It is the retention of only the first-order term which is in analogy to Koopmans' theorem for an independent particle model.[40]

From (1) it is noted that the energy of the state ψ_s^{N-1} is

$$E_S^{N-1} = \langle \psi_s^{N-1} | \bar{\mathcal{H}} | \psi_s^{N-1} \rangle / \langle \psi_s^{N-1} | \psi_s^{N-1} \rangle$$

$$E_S^{N-1} = \langle \psi^N | A_s^+ \bar{\mathcal{H}} A_s | \psi^N \rangle / \langle \psi^N | A_s^+ A_s | \psi^N \rangle$$

It has been assumed that $\bar{\mathcal{H}}\psi^N = E\psi^N$, and therefore the first-order ionization potential of state s is given by eq 2.

$$E_S^{N-1} - E^N = \frac{\langle \psi^N | A_s^+ \bar{\mathcal{H}} A_s | \psi^N \rangle - \langle \psi^N | A_s^+ A_s \bar{\mathcal{H}} | \psi^N \rangle}{\langle \psi^N | A_s^+ A_s | \psi^N \rangle} = \frac{\langle \psi^N | A_s^+ [\bar{\mathcal{H}}, A_s] | \psi^N \rangle}{\langle \psi^N | A_s^+ A_s | \psi^N \rangle} \tag{2}$$

In order to simplify the problem further, it will be assumed that ψ^N based on a finite set of ϕ_i (in this case, the configurations used in the CI calculation) is an eigenfunction of model Hamiltonian $\bar{\mathcal{H}}$, which is the projection of $\mathcal{H}$ in the space spanned by the configurations $\{\phi_i\}$. ψ^N will be an eigenfunction of $\bar{\mathcal{H}}$ if a full CI has been done.

Substitution of (1) into (2) leads to

$$\sum_{ij} C_{si} C_{sj} \langle \psi^N | a_j^+ [\bar{\mathcal{H}}, a_i] | \psi^N \rangle = (E_S^{N-1} - E^N) \sum_{ij} C_{is} C_{js} \langle \psi^N | a_j^+ a_i | \psi^N \rangle \tag{3}$$

If we define

$$V_{ij} = -\langle \psi^N | a_j^+ [\bar{\mathcal{H}}, a_i] | \psi^N \rangle \tag{4}$$

and

$$D_{ij} = \langle \psi^N | a_j^+ a_i | \psi^N \rangle \tag{5}$$

and if we require E_S^{N-1} to be variationally stable with respect to the coefficients C, (3) reduces to a matrix equation

$$\mathbf{V}C = \mathbf{D}C\Delta \tag{6}$$

where $\Delta_{st} = (E^N - E_S^{N-1})\delta_{st}$. The solution of (6) yields the extended Koopmans' theorem ionization potentials. **V** is referred to as the one-particle potential and **D** is the first-order reduced density matrix. The **V** matrix elements may be obtained by recalling the second quantized form of $\bar{\mathcal{H}}$:

$$\bar{\mathcal{H}} = \sum_{ij} \mathbf{f}_{ij} a_i^+ a_j + \sum_{ijkl} \mathbf{g}_{ijkl} a_i^+ a_j^+ a_l a_k \tag{7}$$

where **f** and **g** matrices are the one- and two-electron integrals over configurations. Substitution of (7) into (4) leads to

$$V_{ij} = \sum_k \mathbf{f}_{ik} D_{kj} + \sum_{klm} \mathbf{g}_{iklm} \Gamma_{mlkj} \tag{8}$$

where Γ is the second-order reduced density matrix. In practice, since V_{ij} will only be Hermitian if ψ^N is a true eigenfunction of $\mathcal{H}$, V_{ij} is replaced by $^1/_2(V_{ij} + V_{ji})$ as has been done for atomic EKT calculations.[18] This replacement has been shown to be the best choice to the true self-adjoint matrix **V**.[41]

It is of interest to note that it has been recently proven[42] that if ψ^N is the exact ground-state wave function, then the first ionization potential as calculated by the EKT or MPL method will be exact, as will ψ^{N-1} for the ground state of the ion.

---

(40) See Slater[27] for a discussion of higher order terms in an independent particle model.

(41) Dupré, M. J.; Goldstein, J. A.; Levy, M. *J. Chem. Phys.* **1980**, *72*, 780–781.

(42) Katriel, J.; Davidson, E. R. *Proc. Natl. Acad. Sci. U.S.A.* **1980**, *77*, 4403–4406.

Sch 18640. A New Thiostrepton-Type Antibiotic[1]

M. S. Puar,* A. K. Ganguly,* A. Afonso, R. Brambilla, P. Mangiaracina, O. Sarre, and R. D. MacFarlane[2]

Contribution from the Research Division, Schering Corporation, Bloomfield, New Jersey 07003, and College of Science, Texas A&M University, College Station, Texas 77843.

Received September 26, 1980

Abstract: The structure of a new thiostrepton-type antibiotic, Sch 18640, is established on the basis of degradative and spectroscopic (^{13}C NMR and 600-MHz ^{1}H NMR) studies. In addition, for the first time, ^{252}CF plasma desorption mass spectrometry (^{252}CF-PDMS) has been applied to determine the molecular weight of this class of antibiotics.

Thiostrepton (**1**) produced by *Streptomyces aureus*[3–5] is active against gram-positive bacteria and has found application in veterinary medicine.[6] Its structure was elucidated by using extensive chemical degradations[7] and X-ray crystallographic analysis.[8] Several antibiotics which are closely related to **1** have been isolated, e.g., thiactin[9] bryamicin,[9] thiopeptins,[10] and siomycin.[11,12] Other sulfur-containing antibiotics of similar type are nosiheptide,[13] multhiomycin,[14] and micrococcins.[15]

---

* To whom correspondence should be addressed at Schering Corporation.

(1) After the submission of our results, two reports[11,12] on the structures of similar antibiotics appeared.

(2) Texas A&M University.

(3) Pagano, J. F.; Weinstein, M. J.; Stout, H. A.; Donovick, R. *Antibiot. Annu.* **1955/1956**, 554.

(4) Vandeputte, J.; Dutcher, J. D. *Antibiot. Annu.* **1955/1956**, 560.

(5) Steinberg, B. A.; Jambor, W. P.; Suydam, L. O.; Suriano, A. *Antibiot. Annu.* **1955/1956**, 562.

(6) *Fed. Regist.* **1971**, 36(78), 7583.

(7) Bodanszky, M.; Scozzie, J. A.; Muramatsu, I. *J. Antibiot.* **1970**, *23*, 9 and references cited therein.

0002-7863/81/1503-5231$01.25/0